



Surface roughness analysis of hydrophilic SiO₂/TiO₂/glass nano bilayers by the level crossing approach



E. Daryaei^a, M. Reza Rahimi Tabar^{a,b,*}, A.Z. Moshfegh^{a,c}

^a Department of Physics, Sharif University of Technology, PO Box 11155-9161, Tehran, Iran

^b Institute of Physics, Carl von Ossietzky University, 26111 Oldenburg, Germany

^c Institute for Nanoscience and Nanotechnology, Sharif University of Technology, PO Box 14588-89694, Tehran, Iran

ARTICLE INFO

Article history:

Received 31 May 2012

Received in revised form 7 September 2012

Available online 4 January 2013

Keywords:

AFM images

Hydrophilicity

SiO₂/TiO₂

Stochastic analysis

Etching process

KOH

ABSTRACT

The effect of etching time on the statistical properties of hydrophilic surfaces of SiO₂/TiO₂/glass nano bilayers has been studied using atomic force microscopy (AFM) and a stochastic approach based on a level crossing analysis. We have created rough surfaces of the hydrophilic SiO₂/TiO₂ nano bilayer system by using 26% potassium hydroxide (KOH) solution. Measuring the average apparent contact angle allowed us to assess the degree of hydrophilicity, and the optimum condition was determined to be 10 min etching time. A level crossing analysis based on AFM images provided deeper insight into the microscopic details of the surface topography. With different etching times, it has been shown that the average frequency of visiting a height with positive slope behaves in a Gaussian manner for heights near the mean value and obeys a power law for heights far away from the mean value. Finally, by applying the generalized total number of crossings with positive slope, it was found that the both high heights and deep valleys of the surface have a great effect on the hydrophilic degree of the SiO₂/TiO₂/glass nano bilayer investigated system.

© 2012 Elsevier B.V. All rights reserved.

1. Introduction

Whenever a droplet of liquid such as water is placed on the surface of a substrate, it tries to reach an equilibrium state, and the surface becomes wet [1]. The degree of wetting is determined by the balance between adhesive and cohesive forces. When water spreads and covers a surface in a macroscopic scale, the surface is said to be hydrophilic. The ability to control the degree of hydrophilicity of a solid surface is extremely important and useful in a wide range of technological applications. In the last decade, extensive efforts have been focused on applications of hydrophilic surfaces such as self-cleaning surfaces, anti-fogging mirrors [2] and photocatalysts [3,4].

It has been established that the degree of the wetting and spreading generally depend on both external conditions such as temperature [1] and internal conditions like surface properties. Considering the latter, it has been shown that the surface topography of a substrate [5–7] and surface impurities and contamination as chemical parameters have the most effective role in the hydrophilic degree (or apparent contact angle) of a given hydrophilic surface [8–10].

Today, surface roughness has a vast consideration in science and technology [11,12]; it has an important effect in some physical phenomena such as friction, degrees of hydrophilicity and hydrophobicity, self-cleaning, [13,14] and also improving the mass throughput in microchannel and nanochannel flows [15].

* Corresponding author at: Department of Physics, Sharif University of Technology, PO Box 11155-9161, Tehran, Iran. Tel.: +98 21 6616 4516; fax: +98 21 6601 2483.

E-mail addresses: mohammed.r.rahimi.tabar@uni-oldenburg.de (M. Reza Rahimi Tabar), moshfehg@sharif.edu (A.Z. Moshfegh).

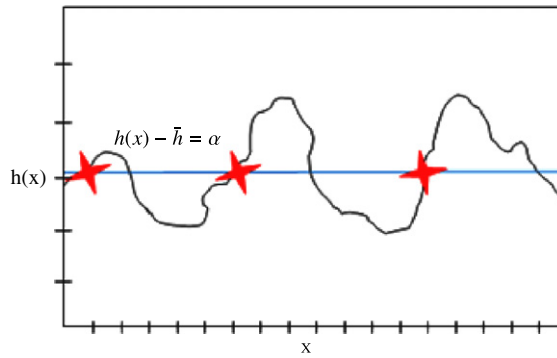


Fig. 1. Schematic positive slope crossing in a fixed α level in a rough surface.

The effect of surface roughness on the contact angle (and hence hydrophilicity) has been studied by many researchers [16]. Morrow carried out pioneering studies of the effect of surface roughness on contact angle, and reported an excellent and extensive set of data [17]. Others have studied the effect of surface roughness on moving contact angles [18–20].

Recently, superhydrophilicity of the $\text{SiO}_2/\text{TiO}_2$ thin film system has been reported by our group and other researchers [21–23]. It was reported that the hydrophilicity of the $\text{SiO}_2/\text{TiO}_2$ nano bilayer films is due to the stable Si-OH groups and that the photocatalytic TiO_2 under-layer maintains the hydrophilicity of the double-layer films by decomposing organic contaminants on the film surface [22]. Moreover, $\text{SiO}_2/\text{TiO}_2$ nano bilayer films exhibit a natural, persistent and regenerable superhydrophilicity without the need of UV light [24].

In this study, first, $\text{SiO}_2/\text{TiO}_2/\text{glass}$ nano bilayer samples were prepared by an RF sputtering technique; then, using 26% potassium hydroxide (KOH) solution, the surface morphology and surface roughness of the layers were examined after different etching times. Their degrees of hydrophilicity were measured after three weeks.

To obtain a deeper insight into the variation of surface topography during the etching process of the hydrophilic $\text{SiO}_2/\text{TiO}_2/\text{glass}$ nano bilayer system, we have applied a level crossing analysis on images obtained by atomic force microscopy (AFM). The level crossing analysis of this data has the advantage that it provides important global properties of a surface. A detailed foundation and the principle of the level crossing analysis approach for rough surfaces have been given in [25]. This stochastic tool has been used to measure the surface roughness for different systems such as the $\text{Co}(3\text{ nm})/\text{NiO}(30\text{ nm})/\text{Si}(100)$ structure used in the magnetic multilayers [26], the effect of annealing temperature on the statistical properties of WO_3 surfaces using AFM [27] and laser-induced silicon surface modification [28]. In addition, this method was also employed in studying the fluctuations of other systems with scale-dependent complexity, such as fluctuations of velocity fields in Burgers turbulence [29], the Kardar–Parisi–Zhang equation in $(d + 1)$ -dimensions [30], and stock markets [31]. As a new application, we have used the level crossing analysis method to describe the effect of etching time on the hydrophilic degree of the $\text{SiO}_2/\text{TiO}_2/\text{glass}$ nano bilayer system.

2. Level crossing analysis: theoretical approach

Level crossing analysis of a stochastic process was first introduced by Rice in 1944 [32]. This method was applied to investigate statistical properties of rough surfaces [25,26]. Consider a surface with size $L \times L$ which has been grown (or etched) in laboratory, so each point on surface such as x has a height $h(x)$; this height function behaves stochastically because the etching process is nondeterministic. Thus, we can apply a level crossing analysis to investigate some general properties of an etched surface.

In the level crossing analysis, we are interested in determining the average frequency (in spatial dimension) of observing a definite value for height function $h - \bar{h} = \alpha$ in growing thin films, v_α^+ , from which one can find the averaged number ($N_\alpha^+ = v_\alpha^+ L$) of crossing the given height in a sample with size L (see Fig. 1) [25]. It can be shown that v_α^+ can be written in terms of joint probability distribution function (PDF) of $h - \bar{h}$ and its gradient. Therefore the quantity v_α^+ carries the whole information of surface lying in joint probability distribution function PDF of height and its gradient [25]:

$$v_\alpha^+ = \int_0^\infty P(\alpha, \dot{h}) \dot{h} d\dot{h}, \quad (1)$$

where $\dot{h} = (h(x + \Delta x) - h(x)) / \Delta x$ and Δx is the differential length scale. Therefore, we can count the number of visiting a definite height such as α and obtain general properties of the joint PDF and all statistical details for a surface. The magnitude of v_α^+ can be related to the magnitude of the three-dimensional (3D) surface area, so its determination is one of the most suitable approaches in experimental surface analysis [26].

As introduced in Refs. [25–31], we can also define the generalized total number of crossings with positive slope, $N_{tot}^+(q)$, as

$$N_{tot}^+(q) = \int_{-\infty}^{+\infty} v_{\alpha}^+ |\alpha|^q d\alpha, \quad (2)$$

where zero moment $q = 0$ (with respect to v_{α}^+) shows the total number of crossings for a height with positive slope $N_{tot}^+ = \int_{-\infty}^{+\infty} d\alpha v_{\alpha}^+$. The moments $q < 1$ will give information about the frequent events while the moments $q > 1$ are sensitive to the rare events. The moment $q = 1$ will measure the total number of crossings of a surface with positive slope multiplied by their heights. So, $N_{tot}^+(q = 1)$ can measure the captive total volume which is the same order of square area of the surface [26].

3. Experimental details

The $2 \times 1 \text{ cm}^2$ glass substrates were cleaned in an ultrasonic bath with high-purity methanol for 10 min and the residual impurities were cleaned with distilled water a few times to ensure surface cleanness. The SiO_2 (20 nm)/ TiO_2 (80 nm) nano bilayers were grown on the cleaned glass substrate by using an RF sputtering deposition technique at room temperature (RT). Two different Ti and Si targets were used under a mixed Ar (60%) and O_2 (40%) gas discharge at total pressure of 10 mTorr.

The deposited SiO_2 (20 nm)/ TiO_2 (80 nm) nano bilayers were subsequently etched by applying a 26% solution of potassium hydroxide (KOH). To prepare the KOH solution, 80 ml DI water, 25 ml propanol (>99.9%, Merck) and 26 g KOH (>99.9%, Merck) were mixed together. The KOH etching process was performed on the prepared bilayers in a constant-temperature bath at 71 °C using clean quartz glassware for various etching times, namely 4, 8, 10 and 12 min, to obtain the optimum etching time as compared with an unetched surface (zero time).

After three weeks, in which the samples had been in normal atmospheric conditions (the relative humidity and temperature were about 60% and 25 °C, respectively), the water apparent contact angle measurements of the KOH etched SiO_2 surfaces of the SiO_2 / TiO_2 /glass nano bi-layer system were made in atmospheric air at room temperature by employing a commercial contact angle meter (Dataphysics OCA 15 plus) with $\pm 1^\circ$ accuracy. To do that, a water droplet was injected on several spots of the surface using a 2 μl micro-injector for obtaining accurate statistical analysis.

In order to determine the apparent contact angle of the clean etched surface (without any surface dirtiness), the etching process was repeated for the optimum etching time and its apparent contact angle was measured again. Surface roughness (the standard deviation of the height values within the given area of AFM image) and surface topography of the samples were characterized by Thermo Microscope Autoprobe CP-Research AFM in air with a silicon tip of 10 nm radius, in contact mode, and the images were digitized into 1024×1024 pixels.

4. Results and discussion

According to our experimental results, the lowest apparent contact angle obtained was $\sim 4^\circ$ for the clean etched surface just after 10 min etching time. Nevertheless, it increased to 21° after three weeks. The observed increasing trend is consistent with a previous study [33]. The behavior of this system is associated with the amount of surface OH species determined by X-ray photoelectron spectroscopy (XPS) reported by our group [23] and others (see, for example, [34]). The surface topography of the whole etched SiO_2 / TiO_2 /glass nano bi-layer system was also investigated by the AFM technique. The three-dimensional AFM image shown in Fig. 2 indicates the average nanostructure size and surface roughness after 10 min etching time.

Fig. 3 shows both changes in the average water apparent contact angle on the surface and changes in the RMS surface roughness of the SiO_2 / TiO_2 /glass nano bilayer after various etching times. The RMS roughness curve indicates that the surface roughness increased from 0.7 nm to 4.8 nm with increasing etching time. Nevertheless, it decreased again to 1.4 nm after 12 min etching time.

It is necessary to note that all contact angle measurements shown in Fig. 3 were performed three weeks after etching of the SiO_2 surface to ensure surface dirtiness, without any surface cleaning process such as UV/ O_3 treatment [33]. The minimum apparent contact angle was determined at 21° after 10 min of etching time. In general, by increasing the etching time, the apparent contact angle decreases, and after 10 min it begins to increase due to reduction of SiO_2 surface roughness. This reduction originates from the decreasing thickness of the SiO_2 layer with increasing etching time. The improvement of the degree of hydrophilicity of the SiO_2 / TiO_2 /glass nano bilayer system by the etching process is the result of topographical change of the etched surface. Increased surface area and topographical changes cause a reduction in the apparent contact angle measurements. This improvement was also observed in other etched substrates [35–37].

There are two conventional theories that discuss the effect of surface roughness on the degree of the hydrophilicity: Wenzel's theory [5] and Cassie–Baxter's theory [6]. The former describes a homogeneous wetting regime in which the droplet completely covers the rough surface without any air pocket while the latter is based on the idea that some entrapped air in a rough heterogeneous surface could enhance its hydrophobicity, recognizing that the water drop is partially sitting on air, not filling the valley. The Wenzel equation is $\cos(\theta_W) = r \cos(\theta_Y)$, $\cos(\theta_W) = r \cos(\theta_Y)$, where θ_W , θ_Y and r are Wenzel's contact angle for rough surface, Young's contact angle for a smooth surface and Wenzel's roughness factor (which

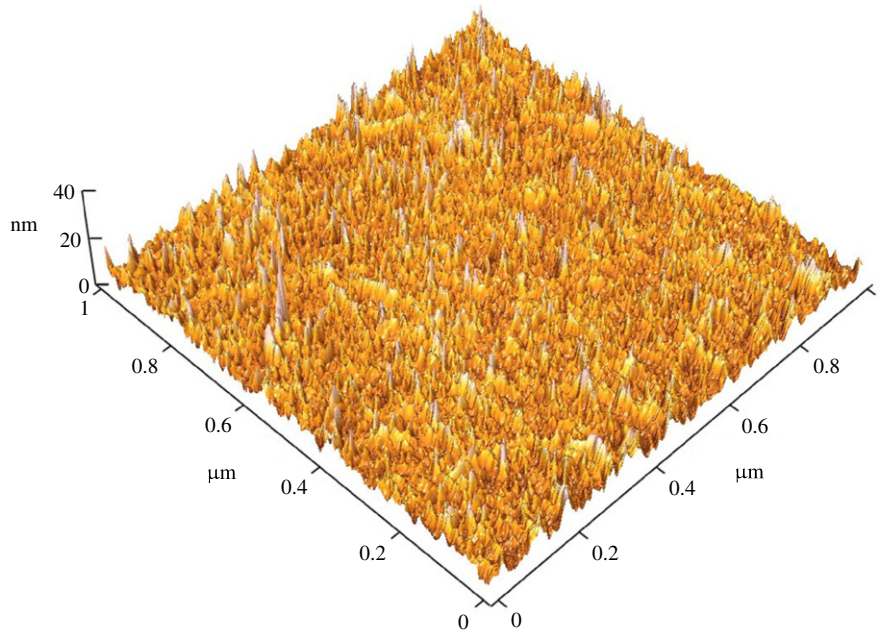


Fig. 2. Three-dimensional AFM image of the SiO₂/TiO₂/glass nano bi-layer surface observed after 10 min etching time.

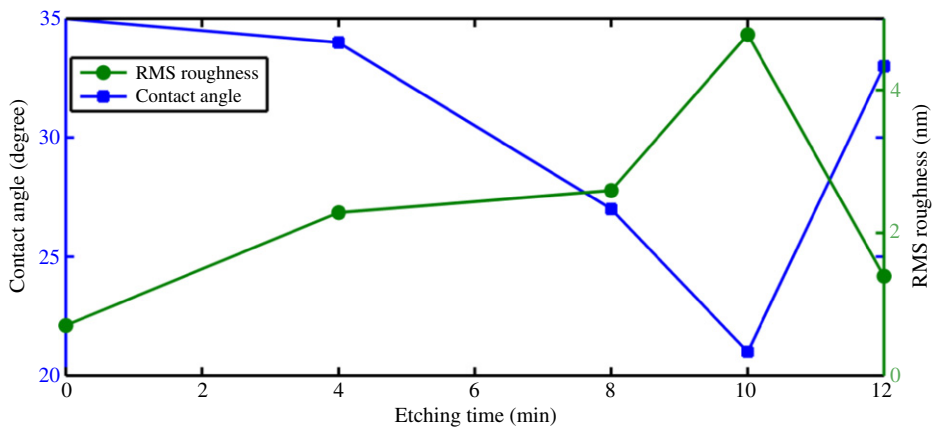


Fig. 3. Variation of average contact angle and the RMS surface roughness of the SiO₂/TiO₂/glass nano bi-layer surface as a function of etching time (all experimental data obtained after three weeks of being kept in atmospheric conditions).

is defined as the ratio of the actual area of rough surface to the geometric projected area), respectively. For a more general and real surface, the Cassie–Baxter equation, $\cos(\theta_{CB}) = rf \cos(\theta_Y) + f - 1$, where θ_{CB} and f are the Cassie–Baxter contact angle for a heterogeneous surface and the fraction of solid surface area wet by the liquid, respectively, can be used. Here the r is the roughness ratio of the wet surface area.

In this study, based on our experimental data analysis, we have used the Wenzel model to describe the degree of the hydrophobicity of the etched surface. This was done by calculating $\cos^{-1}(\cos \theta_W/r)$ for all etched surfaces in order to determine the apparent contact angle for a smooth surface (removing the surface roughness effect). We have obtained the values of the r factor from AFM data analysis. As a result, the contact angle for a smooth surface was found to be in the range from 41° to 47° for r values from 1.20 to 1.32, for all investigated samples. These findings are in good agreement with Wenzel's regime. We believe that, due to surface dirtiness of the SiO₂/TiO₂/glass nano bilayer, we can ignore the hydrophilic role of the TiO₂ sublayer. It is important to note that the obtained r factor is related to both AFM image scale and resolution of each image. We estimated the r factor from the AFM images with size $1 \times 1 \mu\text{m}^2$ and 1024×1024 pixels.

According to water apparent contact angle measurements, the etching rate of the 26% KOH solution at 70 °C used was determined as 15 Å/min by observing the unchanged apparent contact angle after approximately 13 min. This is related to complete etching of the SiO₂ layer (the TiO₂ layer cannot be etched by the KOH solution).

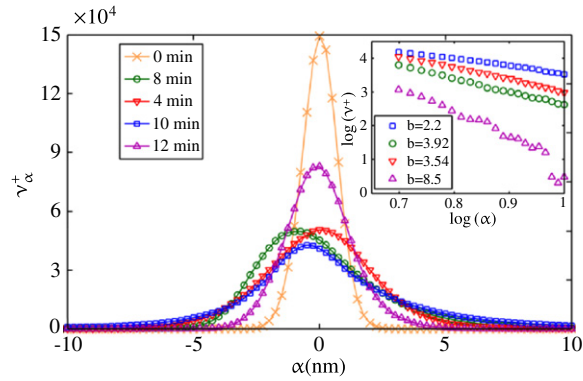


Fig. 4. The average frequency of visiting height $h(x) - \bar{h} = \alpha$ with positive slope ν_{α}^{+} of the etched SiO₂/TiO₂/glass nano bilayer at different etching times as a function of α . Inset: power-law behavior for heights far from mean value (for large α).

To obtain detailed knowledge on the variation of surface topography during the etching process of the hydrophilic SiO₂/TiO₂/glass nano bilayer system, we have applied a level crossing analysis on images obtained by AFM. This procedure was performed on the scanned surfaces as two-dimensional stochastic data as follows. First, the surfaces were cut at different height levels i.e. $h(x) - \bar{h} = \alpha$ [25] in the x and y directions, and then the number of crossing points with positive slope at each level (as shown in Fig. 1) were counted to determine a particular frequency ν_{α}^{+} .

Fig. 4 shows the average frequency of visiting the height α with positive slope, ν_{α}^{+} , as a function of α for different etching times. It is seen that, by increasing the etching time, the average frequency of visiting the height α (ν_{α}^{+}) becomes broader until 10 min and after that it narrows down. In fact, the height dependence of the ν_{α}^{+} function is a Gaussian for small α , and is related to the frequently visited heights near the average height for all surfaces. The standard deviation of each etching time curve (Fig. 4) is related to the corresponding surface roughness obtained by the conventional AFM analysis, as seen in Fig. 3. The shifted peak position of the distribution must be related to the tip convolution effect that was also reported in our previous studies [26,27].

However, there is a definite departure from the Gaussian distribution at large α 's for all etched samples. The average frequency of visiting the heights far from the mean value, where they are related to rare events, have a power law behavior, i.e. $\nu_{\alpha}^{+} \sim \alpha^{-b}$. Here exponent b is related to the surface topography and changes for different etching times. The exponent was obtained by using a least-squares fitting method for different etching times (see the inset of Fig. 4). It varies from 2.2 to 8.5 for, respectively, 10 and 12 min etched samples. The small exponent originates from the increase in number of high heights and deep valleys present on the etched surface.

In fact, the behavior of several physical aspects, at least in some range of length or time scales, is dominated by large and rare fluctuations that are characterized by broad distributions with power-law tails [38]. However, there are several reports of power-law behavior in some nanostructural systems by using AFM data, such as the edge distribution of a nanowire in an inorganic conducting network [39] but, to the best of our knowledge, this is the first report of the observation of a power-law distribution for heights on the hydrophilic surface of SiO₂/TiO₂/glass nano bilayer using AFM images.

In order to get more information about different moments of the probability distribution function, one could calculate the generalized total number of crossings with positive slope, i.e. Eq. (2). For the moment with $q = 0$, it shows the total number of crossings for a height with positive slope. Indeed it shows the total number of an AFM image that is equal to number for all pixels, i.e. $1024 \times 1024 \sim 10^6$. For moment $q = 1$, it will be proportional to the total area of the 3D surface of nanostructure of the etched SiO₂ surface, as reported for the sputtered Co(3 nm)/NiO(30 nm)/Si(100) structure [21]. The higher moments, $q > 1$, give information about the tail of the PDF for a rough surface. For $q \gg 1$, the high values of α will dominate in Eq. (2). Using the power-law expression for level crossing frequency one finds

$$N_{tot}^{+}(q \gg 1) \sim d^{q-b},$$

where d is proportional to the SiO₂ layer thickness as a limit of integration for Eq. (2).

Fig. 5 shows the generalized total number of crossings with positive slope, $N_{tot}^{+}(q)$, for the etched SiO₂/TiO₂/glass nano bilayer surface at different etching times. This function has an increasing trend by increasing the q value in all etched samples. Based on this figure, it was found that the sample with high degree of hydrophilicity had a long tail in the PDF function. This means that the number of high heights and deep valleys are much larger than for other etched surfaces. Therefore, the role of extreme events in the height fluctuations is effective in improving the hydrophilicity of the SiO₂/TiO₂/glass surface.

For some applications in which higher surface areas are useful (such as hydrophilic surfaces of photocatalysts at Wenzel's regime), considering the behavior of $N_{tot}^{+}(q = 1)$ is more appropriate. The increase in $N_{tot}^{+}(q = 1)$ has the same meaning as the increase in both surface area and Wenzel's roughness factor. Indeed, for two surfaces with the same height standard deviation, $N_{tot}^{+}(q = 1)$ can separate the one with a higher surface area.

To correlate the measured macroscopic property (apparent contact angle) with a microscopic property (surface roughness) of the etched surfaces, we have applied the $N_{tot}^{+}(q = 1)$ function as a tool to measure and characterize the

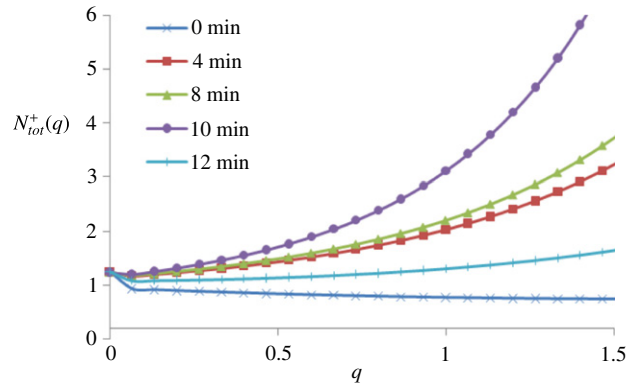


Fig. 5. Generalized total number of crossings with positive slope $N_{tot}^+(q)$ for the etched $\text{SiO}_2/\text{TiO}_2/\text{glass}$ nano bilayer at different etching times.

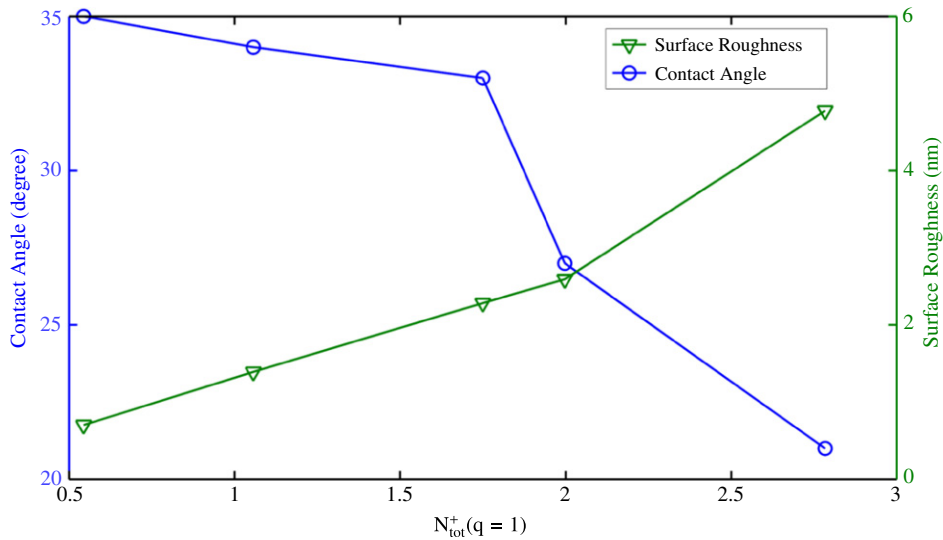


Fig. 6. Variation of surface roughness and contact angle via the generalized function $N_{tot}^+(q = 1)$.

three-dimensional etched surface. Fig. 6 shows the variation of surface roughness and contact angle of the etched surface via the generalized total number of crossing with positive slope at $q = 1$. It is clear that the contact angle is reduced with increasing $N_{tot}^+(q = 1)$, whereas the surface roughness of the SiO_2 etched layer has an increasing trend, but not in a linear fashion. Thus, we can consider $N_{tot}^+(q = 1)$ as another quantity to evaluate the surface morphology of the samples. It is necessary to note that, in this figure, all the points in both graphs are arranged based on increasing $N_{tot}^+(q = 1)$ value, and not arranged by the etching time duration.

5. Conclusions

Nanoscale roughness was generated on the hydrophilic surfaces of sputtered $\text{SiO}_2/\text{TiO}_2/\text{glass}$ nano bilayers by applying 26% KOH solution. The results of apparent contact angle measurements and AFM analysis have shown that extreme events in nanoscale surface roughness significantly increase the degree of surface hydrophilicity. These microscopic changes in surface topography contribute to increasing the hydrophilicity. A behavioral change from increasing hydrophilicity to decreasing hydrophilicity was observed after 10 min of etching time. We have found that the hydrophilicity degree of a surface can be improved by using a simple etching process.

To obtain a deeper insight into the variation of surface topography during the etching process of the hydrophilic $\text{SiO}_2/\text{TiO}_2/\text{glass}$ nano bilayer system, we have applied a level crossing analysis on images obtained by AFM. We have investigated the role of etching time, as an external parameter, to control the statistical properties of a rough SiO_2 surface. Moreover, by using the level crossing analysis, we have obtained an optimum etching time (10 min) to have the highest hydrophilic degree. The average frequency of visiting the height α with positive slope, ν_α^+ , was calculated for different etching times, and it was found that the height dependence of ν_α^+ is Gaussian for heights near the mean value and that it obeys a power law for heights far from the mean value. Applying the generalized total number of crossings with positive

slope, $N_{tot}^+(q)$, we have found that the high heights and deep valleys of the surface have a great effect on the hydrophilic degree of SiO₂/TiO₂/glass nano bilayers.

Acknowledgments

We would like to thank Dr. G.R. Jafari, Dr. R. Azimirad and Dr. O. Akhavan for useful discussions, and F. Vaseghiniya for providing AFM images. A.Z.M. acknowledges financial support from Sharif University of Technology.

References

- [1] For a recent review, see D. Bonn, J. Eggers, J. Indekeu, J. Meunier, E. Rolley, *Rev. Modern Phys.* 81 (2009) 739.
- [2] A. Fujishima, K. Hashimoto, T. Watanabe, TiO₂, Photocatalysis, Fundamentals and Applications, BKC Inc., Tokyo Japan, 1999.
- [3] A. Fujishima, X. Zhang, D.A. Tryk, *Surf. Sci. Rep.* 63 (2008) 515.
- [4] A.Z. Moshfegh, *J. Phys. D: Appl. Phys.* 42 (2009) 233001.
- [5] R.N. Wenzel, *Ind. Eng. Chem.* 28 (1936) 988;
R.N. Wenzel, *J. Phys. Colloid Chem.* 53 (1949) 1466.
- [6] A.B.D. Cassie, S. Baxter, *Trans. Faraday Soc.* 40 (1944) 546.
- [7] D. Quéré, *Rep. Progr. Phys.* 68 (2005) 2495.
- [8] K. Okada, T. Tomita, Y. Kameshima, A. Yasumori, K.J.D. MacKenzie, *J. Colloid Interface Sci.* 219 (1999) 195.
- [9] T. Soeno, K. Inokuchi, S. Shiratori, *Appl. Surf. Sci.* 237 (2004) 539.
- [10] R. Azimirad, N. Naseri, O. Akhavan, A.Z. Moshfegh, *J. Phys. D: Appl. Phys.* 40 (2007) 1134.
- [11] A.L. Barabási, H.E. Stanley, *Fractal Concepts in Surface Growth*, Cambridge University Press, 1995;
G.R. Jafari, S.M. Fazeli, F. Ghasemi, S.M. Vaez Allaei, M. Reza Rahimi Tabar, A. Irajizad, G. Kavei, *Phys. Rev. Lett.* 91 (2003) 226101.
- [12] S. Davies, P. Hall, *J. Roy. Stat. Soc. B* 61 (1999) 3.
- [13] A.G. Peressadko, N. Hosoda, B.N.J. Persson, *Phys. Rev. Lett.* 95 (2005) 124301.
- [14] Y.P. Zhao, L.S. Wang, T.X. Yu, *J. Adhes. Sci. Technol.* 17 (2003) 519.
- [15] M. Sbragaglia, R. Benzi, L. Biferale, S. Succi, F. Toschi, *Phys. Rev. Lett.* 97 (2006) 204503.
- [16] M. Sahimi, *Flow and Transport in Porous Media and Fractured Rock*, 2nd ed., Wiley-VCH, Weinheim, 2011, Chapter 14.
- [17] N.R. Morrow, *Ind. Eng. Chem.* 62 (1970) 32;
N.R. Morrow, *J. Can. Pet. Technol.* 14 (1975) 42;
N.R. Morrow, *J. Can. Pet. Technol.* 15 (1976) 49.
- [18] J.F. Joanny, P.G. de Gennes, *J. Chem. Phys.* 81 (1984) 552.
- [19] Y. Pomeau, J. Vannimenes, *J. Colloid Interface Sci.* 104 (1985) 447.
- [20] J.F. Joanny, M.O. Robbins, *J. Chem. Phys.* 92 (1990) 3206.
- [21] M. Nakamura, *Thin Solid Films* 496 (2006) 131.
- [22] M. Nakamura, M. Kobayashi, N. Kuzuya, T. Komatsu, T. Mochizuka, *Thin Solid Films* 502 (2006) 121.
- [23] S. Ganjoo, R. Azimirad, O. Akhavan, A.Z. Moshfegh, *J. Phys. D: Appl. Phys.* 42 (2009) 025302.
- [24] S. Permpoon, M. Houmard, D. Riassetto, L. Rapenne, G. Berthomé, B. Baroux, J.C. Joud, M. Langlet, *Thin Solid Films* 516 (2008) 957.
- [25] R. Friedrich, J. Peinke, M. Sahimi, M. Reza Rahimi Tabar, *Phys. Rep.* 506 (2011) 87;
F. Shahbazi, S. Sobhanian, M. Reza Rahimi Tabar, S. Khorram, G.R. Frootan, H. Zahed, *J. Phys. A: Math. Gen.* 36 (2003) 2517.
- [26] P. Sangpour, G.R. Jafari, O. Akhavan, A.Z. Moshfegh, M. Reza Rahimi Tabar, *Phys. Rev. B* 71 (2005) 155423.
- [27] G.R. Jafari, A.A. Saberi, R. Azimirad, A.Z. Moshfegh, Rouhani, *J. Stat. Mech.* (2006) P09017.
- [28] M. Vahabi, G.R. Jafari, N. Mansour, R. Karimzadeh, J. Zamiranvari, *J. Stat. Mech.* (2008) P03002.
- [29] S. Movahed, A. Bahraminasab, H. Rezazadeh, A.A. Masoudi, *J. Phys. A: Math. Gen.* 39 (2006) 3903.
- [30] A. Bahraminasab, M. Sadegh Movahed, S.D. Nassiri, A.A. Masoudi, Preprint [condmat/0508180](#) (2005).
- [31] G.R. Jafari, M.S. Movahed, S.M. Fazeli, M. Reza Rahimi Tabar, S.F. Masoudi, *J. Stat. Mech.* (2006) P06008;
F. Shayeganfar, M. Hölling, J. Peinke, M. Reza Rahimi Tabar, *J. Physica A* 391 (2012) 209.
- [32] S.O. Rice, *Bell System Tech. J.* 23 (1944) 282.
- [33] S. Takeda, M. Fukawa, *Mater. Sci. Eng. B* 119 (2005) 265.
- [34] S. Takeda, M. Fukawa, *Thin Solid Films* 444 (2003) 153.
- [35] D. Tahn, T. Kim, H. Yoon, M. Choi, K. Shin, K.Y. Suh, *Langmuir* 26 (2010) 2240.
- [36] W. Zenglin, L. Zhixin, H. Yue, W. Zhixiang, *J. Electrochem. Soci.* 158 (11) (2011) D664.
- [37] K. Dongseob, L. Sangmin, H. Woonbong, *Curr. Appl. Phys.* 12 (2012) 219 15.
- [38] L.A.N. Amaral, S.V. Buldyrev, S. Havlin, M.A. Salinger, H.E. Stanley, *Phys. Rev. Lett.* 80 (1998) 1385;
G.M. Viswanathan, S.V. Buldyrev, S. Havlin, M.G.E. da Luz, E.P. Raposo, H.E. Stanley, *Nature (London)* 401 (1999) 911;
A.L. Barabási, R. Albert, *Science* 286 (1999) 509.
- [39] J. Strle, D. Vengust, D. Mihailovic, *Nano Lett.* 9 (2009) 1091.